Distribution Category:
General, Miscellaneous,
and Progress Reports
(UC-700)

ANL/ACTV-91/5

ANL/ACTV--91/5

DE92 015168

ARGONNE NATIONAL LABORATORY
9700 South Cass Avenue
Argonne, Illinois 60439

INTRINSIC-SURFACE-TAG IMAGE AUTHENTICATION

by

R. G. Palm and A. DeVolpi*

Reactor Engineering Division

December 1991

Work sponsored by
U. S. Department of Energy
Office of Arms Control

MASTER

*Engineering Physics Division

TABLE OF CONTENTS

LIST OF FIGURES

LIST OF TABLES

Intrinsic-Surface-Tag Image Authentication

by

R. G. Palm and A. DeVolpi

Abstract

The objective of this work is to further the development of a unique treaty limited item (TLI) intrinsic surface tag for arms control applications. This tag's unique feature is the ability to capture the sub-micron scale topography of the TLI surface. The surface topography is captured by plastic castings of the surface as digitally imaged by an electron microscope. Tag authentication is accomplished by comparing digital casting images obtained in two different inspections. Surface replication experiments are described, as these experiments form the basis for the authentication algorithm. Both the experiments and the authentication algorithm are analyzed using the modulation transfer function. Recommendations for future improvements in tag authentication are also suggested by the modulation transfer function analysis.

I. INTRODUCTION

The intrinsic-surface tag is a unique tamper-resistant identifier that is simple, inexpensive, and developed sufficiently for immediate implementation. Another term for this tag is "fingerprinted-registration" because of its similarity to well-understood practices of fingerprinting and vehicle registration. The three major elements of the concept are bar codes for registration of a TLI, surface features of the TLI for unique identification, and fingerprints for a verifiable record. Depending upon treaty requirements, there are several ways to implement the concept.

The bar codes are used to "register" each treaty-limited item. Bar codes can be easily read in the field with portable scanners. The data for each item can then later be accurately and quickly transferred into the computerized treaty database.

Markings or features on the surface of the TLI -- natural surface-roughness, existing, or added inscriptions -- provide unique signatures. When greatly magnified, no two surfaces appear the same. This concept was initiated at the Western European Union and has been under development at the ISPRA Joint Research Laboratory of Euratom.

To authenticate the surface signature, the idea of making and verifying a plastic casting fingerprint has been developed at Argonne National Laboratory. The plastic casting is easy to make. After a fingerprint casting is made, it can be sent to a central laboratory or repository for analysis and storage. Each treaty party, alliance, and/or a unified verification organization could have such a laboratory. At this facility there would be an electron microscope that would magnify the casting image and digitize the three-dimensional impression.

A comparison would be made of the casting fingerprint obtained during the baseline period and the one made during a subsequent short-notice inspection. It is possible for the initial surface casting to be made by the equipment owner **without** an inspecting party being present. This self-application capability has important consequences from the viewpoint of cost-reduction and burden-sharing.

The purposes of this report are (1) to describe intrinsic-surface tag replication experiments, (2) to present the digital image comparison procedures, and (3) to provide criteria for authentication. First, the experimental method used to attempt tag replication is briefly described. The replicas produced were positives of an original tag surface, and they exhibited visually-obvious, random, generic defects in the bright areas of their images. Then, digital scanning electron microscope (SEM) images of original tags are compared with those of replica tags. Digital images of two castings from the same tag are also subjected to the same comparisons. The image comparison procedure was formulated to emphasize bright-feature replica defects. The image comparisons result in a numerical tag score that indicates the degree of image agreement and authenticates the tag if the agreement is good. Finally, the replication results are placed in the framework of the modulation transfer function (MTF), which provides both a first-principle approach to analyzing image-reproduction accuracy and a means to maximize the differences between real and replica images.

II. REPLICATION METHOD

For this study, the original surface was a one-centimeter diameter, 60%Au-40%Pd disk. The disk was scratched in one direction with 80-grit sandpaper scratches. Rows of micro-indent marks were also placed on the disk to facilitate subsequent azimuthal alignment in the SEM.

The basic replication method is based upon standard replication techniques used by electron microscopists.[1,2] Replicated tag surfaces were made according to the steps shown in Fig. 1. The first step was to make a cellulose-acetate casting (negative) of the original surface. This negative was separated from the original, turned over and sputter-coated with 500 to 1000 nm of gold to form a positive. After sputter-coating, the negative and positive were placed in a special SEM mount, so the cellulose acetate was above the gold. Then the mount was placed in acetone to dissolve the cellulose acetate negative. After drying, the positive replica gold-foil surface was examined in the SEM along with the original Au-Pd surface. Both the gold and the gold-palladium surfaces were essentially free of surface oxides that can degrade the ultimate resolution of the SEM. Therefore, surface features for either material were equally well resolved. Digital images of these surfaces were obtained in the slow-scan mode at magnifications up to 5500X. In order to obtain the best agreement between images, it was important to preserve azimuthal alignment between the SEM beam, specimen, and secondary-electron detector. Alignment of the specimens in the SEM was kept within ± 2 degrees, by scribing the SEM screen with crayon marks at the center of the cross pattern formed by the micro-indent marks. This degree of alignment was sufficient to obtain high image correlation between different specimens.

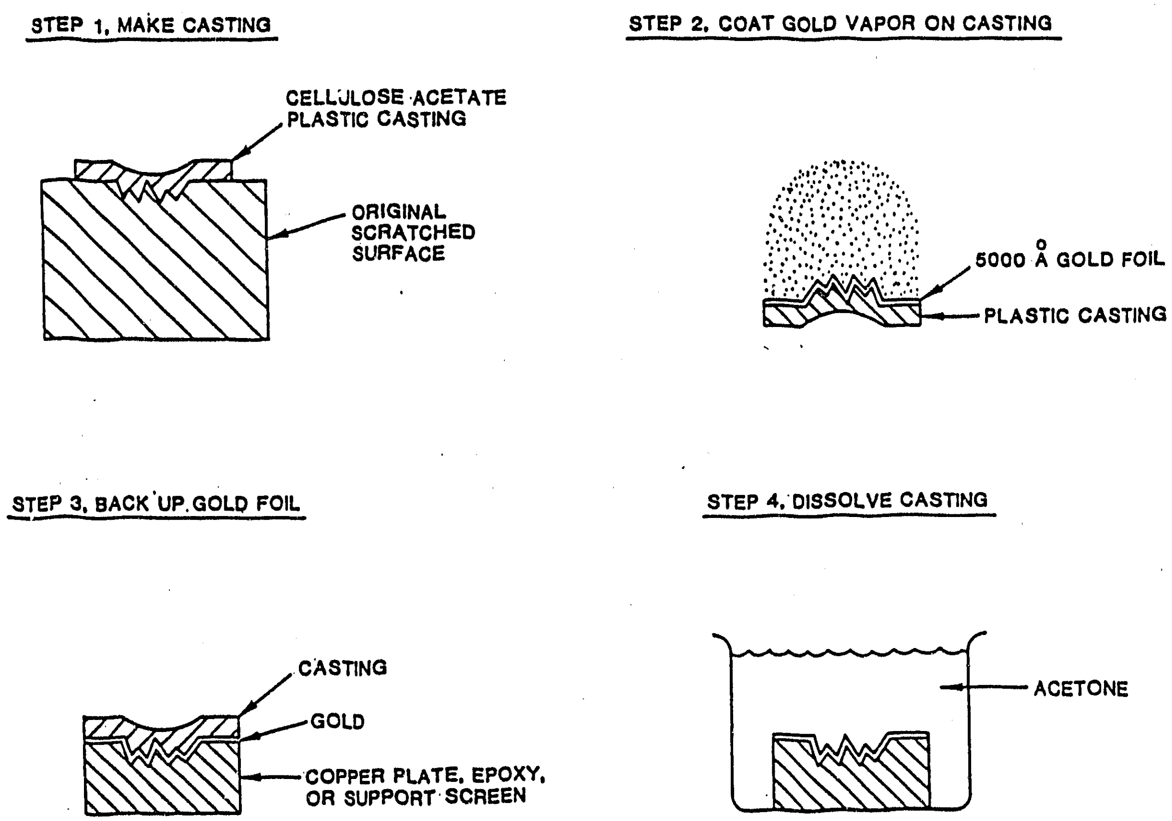

Figure 1. Replication Method

III. ORIGINAL AND REPLICA IMAGE COMPARISONS

This section describes how original-replica as well as casting-image pairs are analyzed for tag comparison.

A. Analysis Steps

1. Image Registration and Correlation of Gray-Scale Images

Before two digital images derived from the same surface can be compared, a certain amount of processing is necessary to register them. Registration is needed to correct for small translation, magnification and azimuthal misalignments between the two images. For each digital image, a gray-scale value is associated with each address (pixel) in the image. So for digital image A, A(x,y) is the gray-scale value of the pixel associated with each (x,y) address. In this study, each pixel had 256 possible gray-scale intensity values. When authenticating two digital images, A and B, registration is achieved when each (x,y) address of both images corresponds to the same point on the surface being compared. A measure of image registration, known as the linear correlation coefficient (LCC), is maximized at the optimum registration.[3] The maximum LCC can also be used to provide a tag score. An LCC of 1.0 indicates perfect agreement, while an LCC near 0.0 would be expected for totally uncorrelated images from two different surfaces. Details of the registration process and LCC determination as implemented by the Semper image-registration software are described in Appendix I. Semper is a trademark of Synoptic's Ltd., Cambridge, United Kingdom.

Figures 2a and 2b compare two sets of gray-scale images. Figure 2a is a comparison of two casting images from the same original, and these two images have an LCC of 0.919. Figure 2b is a comparison of an original with an attempted replica, and these two images have an LCC of 0.875. Visual inspection shows that the images in I 2a agree better in the brighter areas that represent high areas in the surface. However, there is only a 5% difference in the LCC discrimination ability, so the LCC provides a crude tag score with limited discrimination. Note that Figs. 2a and 2b also present another image comparison statistic called the local sum. This statistic is described in a subsequent section.

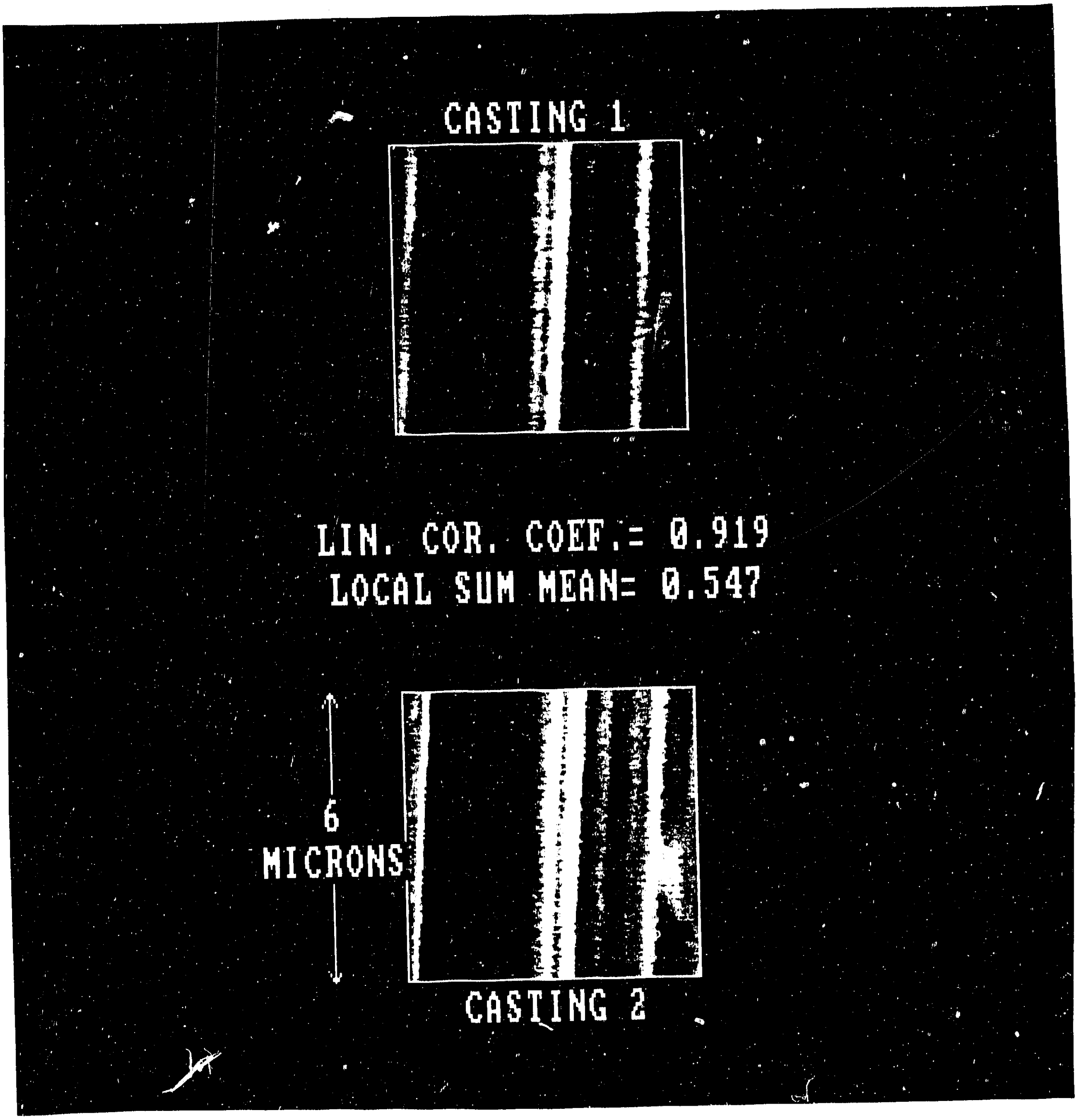

Figure 2a. Casting Image Comparison Using Linear Correlation Coefficient and Local Sum Mean

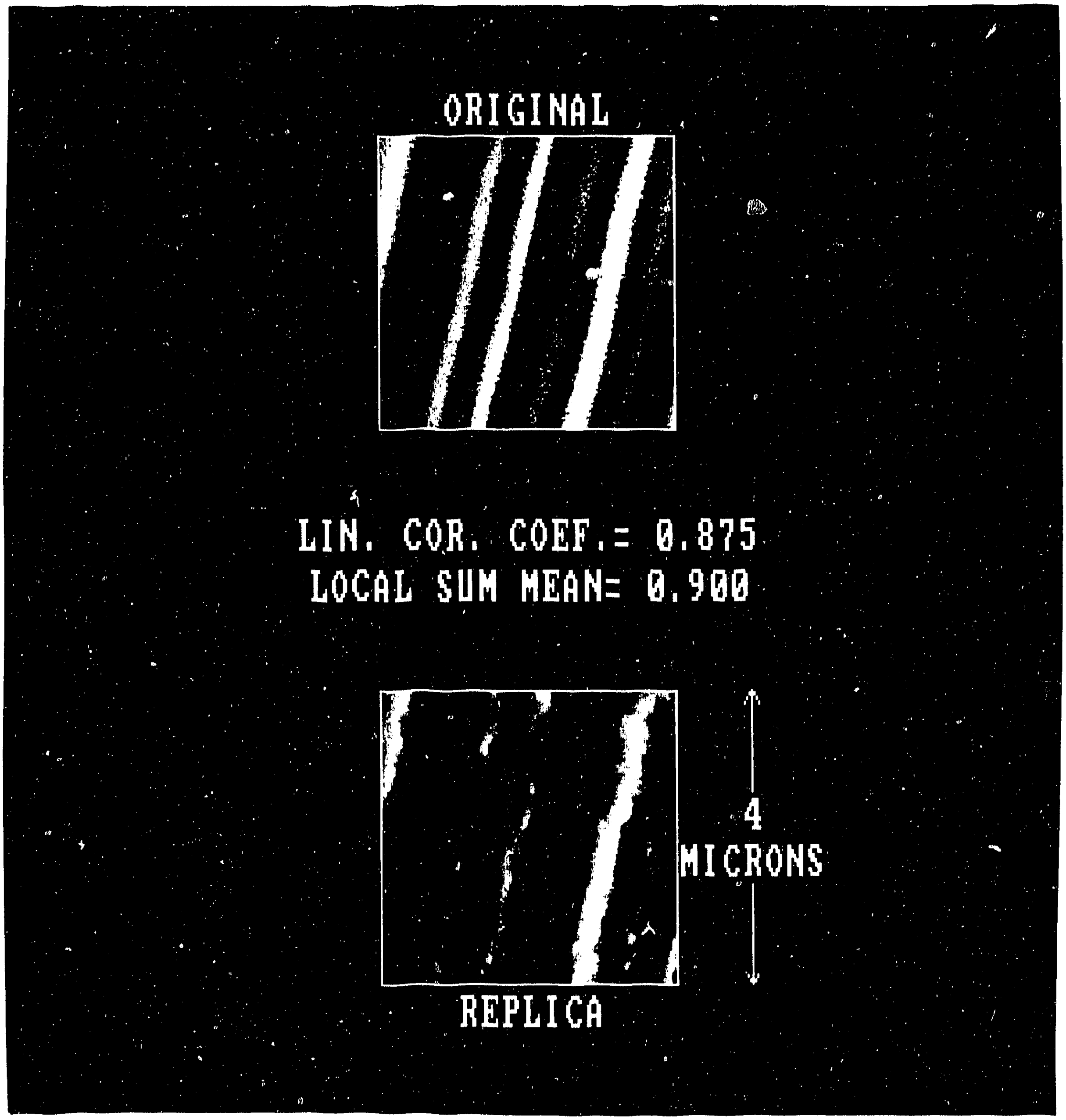

Figure 2b. Original-Replica Image Comparison Using Linear Correlation Coefficient and Local Sum Mean

Figure 3 presents another pair of images of an original and replica illustrating similar disagreement among the brightest pixels. For illustrative purposes, this set is repeated twice in the top half of Fig. 3. It is possible to extract rectangular sub-regions around the brightest areas and determine the correlation between sub-regions. Two sets of sub-regions are correlated in Fig. 3. These sub-region sets are shown in the lower part of this figure, and the sources of the sub-regions are marked in the top part. Figure 3 shows the broad sub-region shown in the lower left of Fig. 3 has a LCC of 0.828. This value is only 0.5% less than the LCC of 0.832 for the whole image comparison. In the lower right is a very narrow sub-region set; it had a low LCC of 0.414. Therefore, visual observation of the disagreement is confirmed by the LCC if small enough sub-regions near the bright areas can be chosen for correlation. However, choosing and correlating all such small sub-regions in the two images being compared is a difficult process to implement.

From examining Figs. 2 and 3 it is apparent the LCCs reported on the whole images are a rather insensitive indicator of image disagreement. A more sensitive and simple means to authenticate a tag image based upon its brightest areas can be formulated.

2. Binary Image Comparison

Because the differences in the gray-scale images were clustered near the brightest pixels, it is necessary to emphasize the brightest pixels before comparing the images. A standard image-analysis technique used to emphasize features with a common gray-scale intensity range is to form a thresholded binary image from the gray-scale image. Each pixel in the binary image is set to one if the corresponding pixel in the gray-scale image falls in the intensity range of interest. Otherwise, the binary pixel is set to zero. In this case, each binary image pixel value is set to one if the corresponding gray-scale pixel is in the brightest 15% set of pixels. The brightness thresholded binary images A_b and B_b are then derived from their respective gray-scale brightness images A and B. A_b and B_b can be compared to determine a numerical score for tag comparison. Figure 4 shows binary images derived from an original (top) and a replica (bottom). Inspection of Fig. 4 shows the replica binary, bright sub-regions to be wavy and discontinuous compared to the original's binary sub-regions. Therefore, the brightness-threshold process visually captures the differences between the original and replica. Appendix I provides a more detailed description of the binary image processing and its implementation within the Semper software.

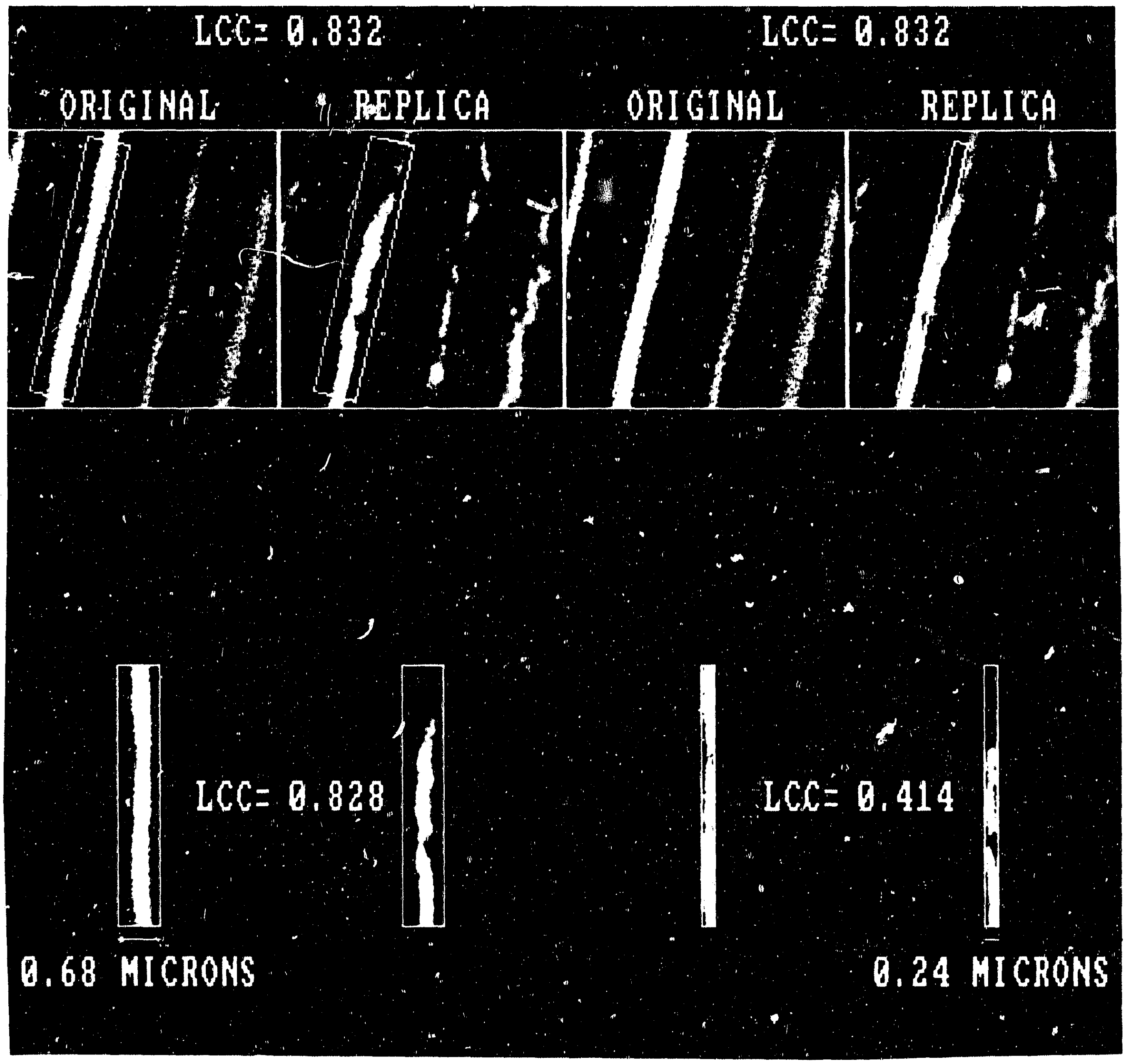

Figure 3. Linear Correlation Coefficients for Sub-Regions Around Bright Areas

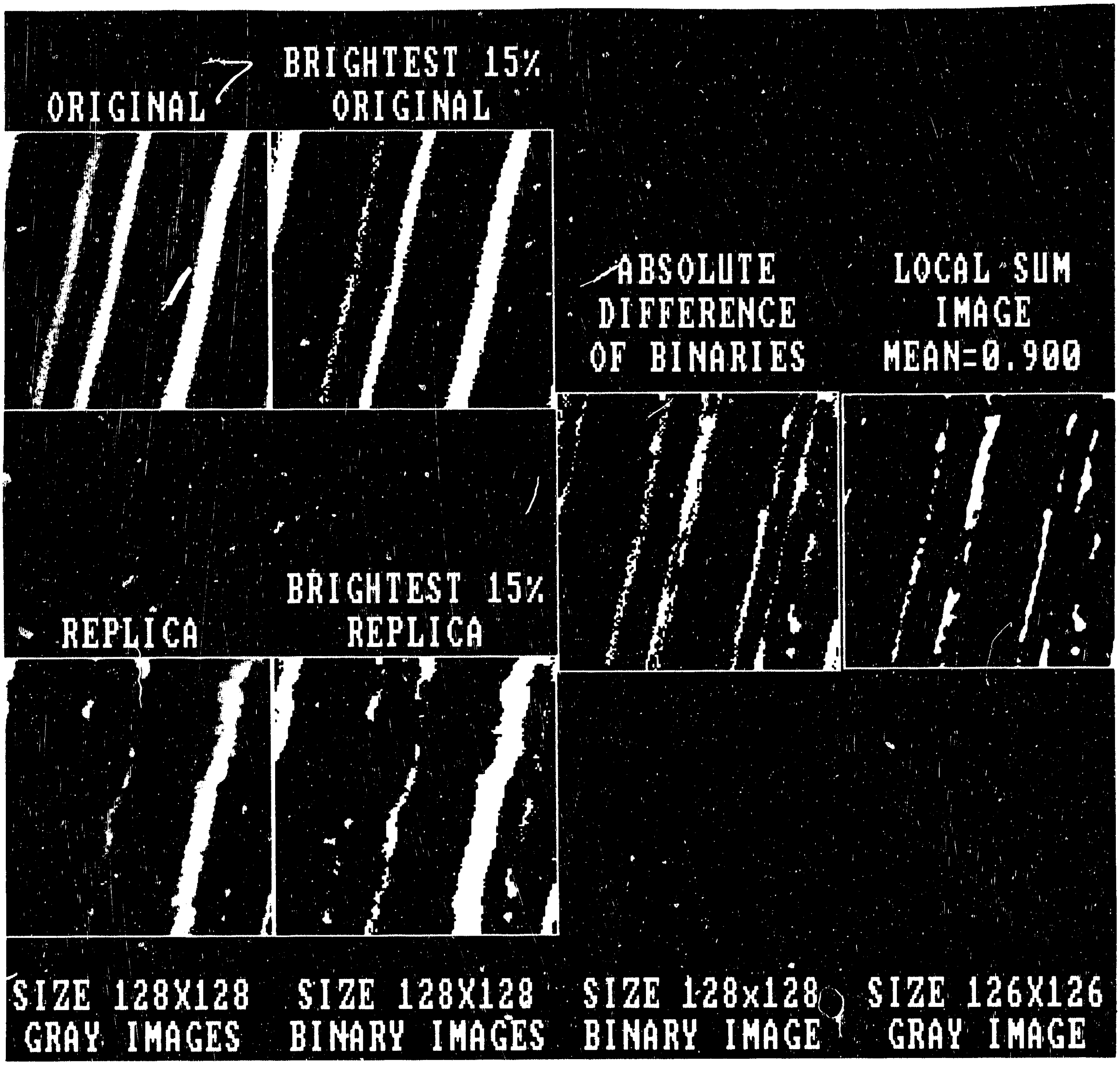

Figure 4. First Illustration of Steps in Calculating the Local-Sum Image

a. Absolute Difference Image

A simple way to compare the binary images is to form the absolute-difference image C_b from A_b and B_b according to:

$$C_b(x,y) = |A_b(x,y) - B_b(x,y)|$$

The pixels in image C_b are set to one for the pixels in A_b and B_b that disagree. Otherwise the pixels are set to zero. Therefore, image C_b gives a binary indication of the pixels in A_b and B_b that disagree. A possible tag acceptance criterion derived from C_b is simply its mean. Low means indicate good agreement. The mean of C_b can span from zero (perfect agreement) to one.

b. Local-Sum Image

Another way to view C_b is to form a local-sum image. This local-sum image also presents a gray-scale rendition of the local disagreement between images A_b and B_b. The local-sum image, referred to as image D, renders the degree of disagreement of local p by p pixel clusters in C_b. Each local-sum pixel D(x,y) is produced by summing each pixel $C_b(x,y)$ with its p^2-1 nearest neighbors and placing the sum in D(x,y). The pixels within a distance p-2 of the border of C_b can't be summed over p^2 pixels. Therefore, if the image C_b has dimensions M by N, the local-sum image has dimensions M-p+1 by N-p+1. The pixel values of the local-sum image can span the range from 0 (complete agreement) to p^2 (complete disagreement).

Figure 4 shows the local-sum image formed by an original and a replica. Disagreement amongst the brightest pixels is rendered by the local-sum image gray-scale. For a p=3 local-sum image shown in Fig. 4, the local-sum pixel values range from 0 to 9. The tag-acceptance criteria derived from local-sum image D is simply its mean. Low means indicate good agreement. The mean of D is about nine times the mean of C_b for 3 by 3 local-sum images. The local-sum mean for this original-replica comparison is 0.900.

Figure 5 illustrates the binary images for two castings of the same original surface. Inspection of Fig. 5 shows the binary images to be similar. This similarity results in a low value of the local-sum mean. The local-sum mean for this original-replica comparison is 0.547.

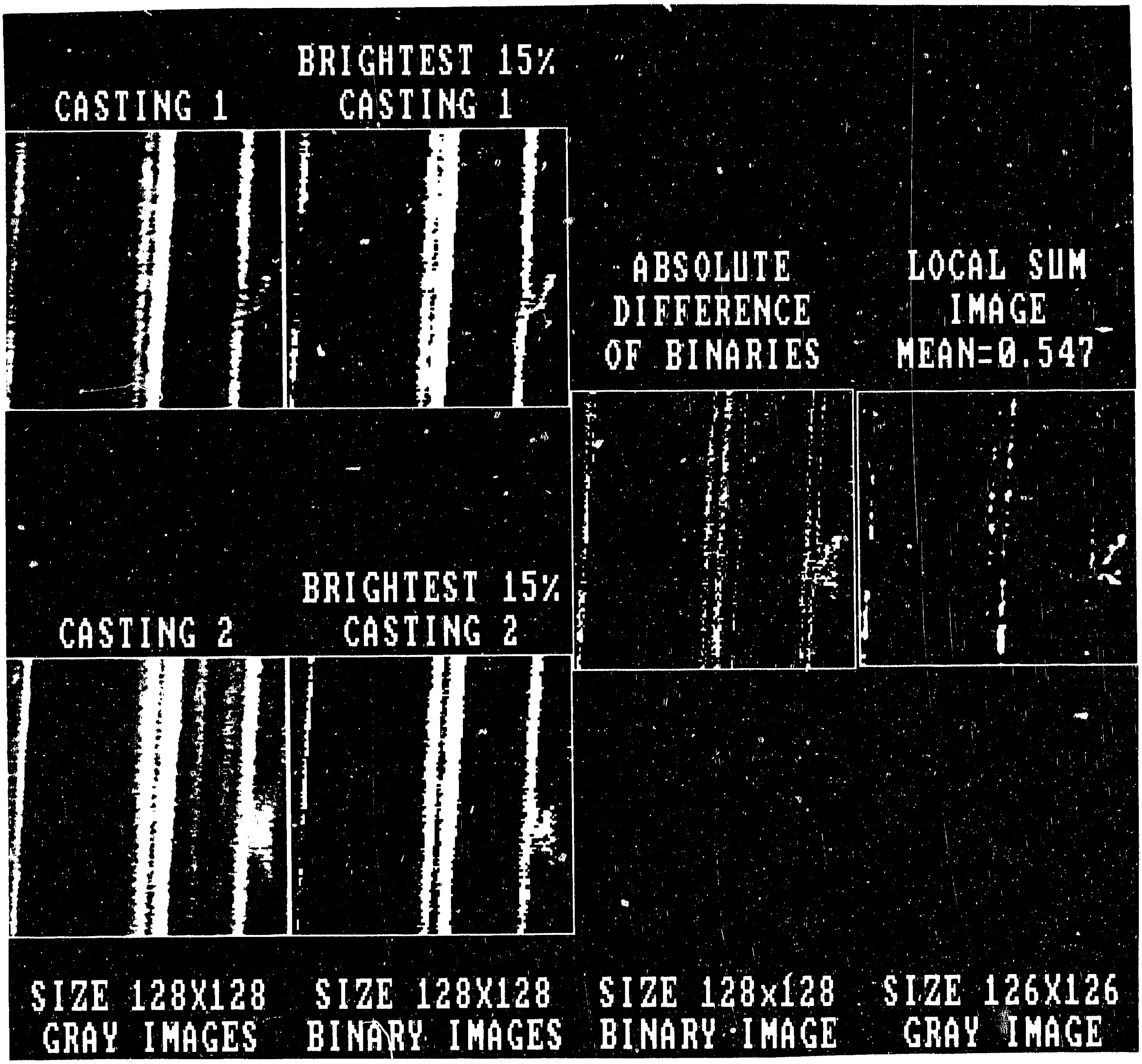

Figure 5. Second Illustration of Steps in Calculating the Local-Sum Image

Figures 2a and 2b show the gray images used to calculate the local-sum means in Figs. 4 and 5, along with their LCC values. Even though the LCC's differed by only 5% the local-sums differ by 64%. Therefore, the local-sum mean is a good discriminator of the bright ridge-line defects present in replica images, but not present in images of two castings from the same original.

A quantitative test based upon the binary images is dependent upon the threshold limit used to derive the binary images. The brightness threshold limit of 15% was empirically determined to provide the best quantitative discrimination between original surfaces and replicas.

B. Tentative Acceptance Criteria for Tag Sub-Areas

Table I presents LCC and local-sum mean for the two types of image comparisons used to formulate the empirical tag-acceptance criteria. The first kind of image comparison was for two castings taken from the same original tag. Acceptance criteria for the castings were formulated, so all of the casting image comparisons had passing scores for castings acquired at a SEM magnification of 4000X. The second kind of image comparison compared original tags with positive replicas of the original. The acceptance criteria could be formulated, so that all but one of these image comparisons acquired at 5500X did not meet the acceptance criteria.

Based upon the images examined for this study, empirical tag-acceptance criteria can be formulated. Sub-area images are accepted as from a genuine tag if the LCC > 0.7 and the local-sum mean is < 0.6. Since the image-registration process computes the LCC to determine the best registration of the two images, it is determined before the local-sum mean. Therefore, if the LCC of a sub-area is < 0.7, the sub-area fails to pass, and the local-sum mean need not be calculated. Figs. 2 and 3 show that it is relatively easy to satisfy the LCC part of the acceptance criteria. However, meeting the local-sum criteria is more demanding; only two images with their brightest pixels in registration can satisfy it.

One further tag-acceptance criterion must be developed as more data are examined. This criterion would evaluate the number of sub-area passes and fails to provide a overall tag-score. An example of an overall tag score criterion would be to accept the tag as genuine if 80% of the sub-areas passed, out of 1000 sub-areas examined.

TABLE I					
NUMERICAL IMAGE COMPARISON RESULTS					
Image #1 file number	Image #2 file number	Magnification	Linear correlation coefficient	Mean, local-sum image	Mean, absolute difference image
5242ca	5241ca	4000	0.907	0.571	0.0631
5244ca	5243ca	4000	0.919	0.547	0.0602
5225ca	5226ca	2000	0.869	0.566	0.0615
5221ca	5222ca	2000	0.895	0.451	0.0500
5223ca	5224ca	2000	0.757	0.795	0.0870
5227ca	5228ca	2000	0.915	0.598	0.655
5201ca	5202ca	700	0.922	0.407	0.0453
5111or	5112rp	5500	0.875	0.844	0.0966
5121pr	5122rp	5500	0.881	0.947	0.1083
5165or	5168rp	5500	0.756	1.154	0.1296
5155or	5158rp	5500	0.918	0.601	0.0663
5101or	5102rp	5500	0.832	0.838	0.0943
5101or	5103rp	5500	0.606	1.172	0.1300
5101or	5104rp	5500	0.669	1.163	0.1277
5193or	5194rp	700	0.898	0.410	0.0452
5193or	5195rp	700	0.898	0.408	0.0452

ca = casting; or = original; rp = replica

Image comparisons at lower magnifications are also presented in Table I. These comparisons were not used to formulate the acceptance criteria, but are referred to in a later section discussing the importance of using the proper SEM magnification in tag authentication.

Figure 6 shows the results of three attempts to replicate the same surface. All the attempts failed to meet the acceptance criteria. Only one of these replication attempts passed the LCC part of the acceptance criteria. For this set of replicas, the LCC and the local-sum mean varied inversely. More work needs to be done to see if this inverse relationship holds for large numbers of original-replica comparisons.

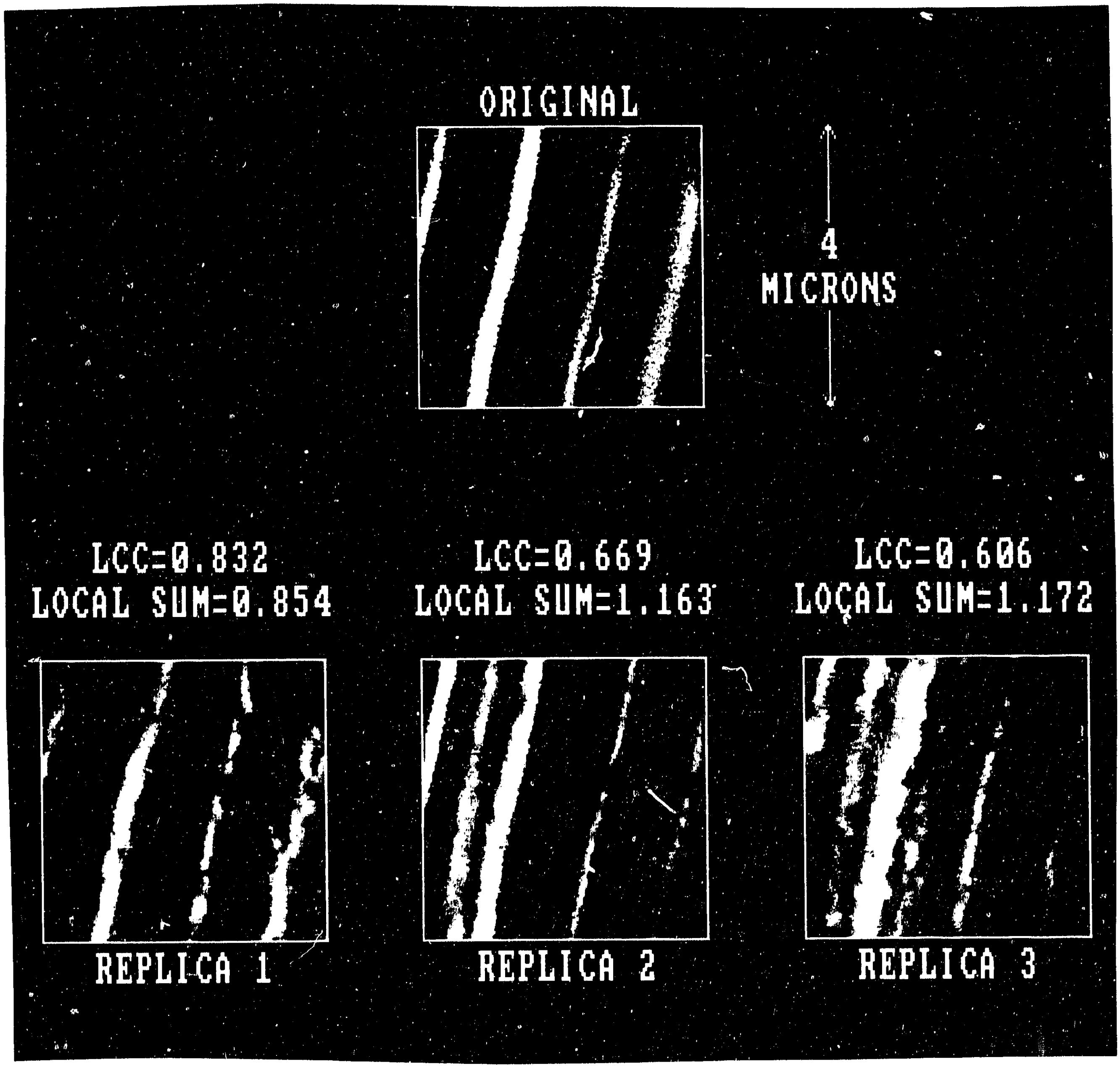

Figure 6. Comparison of an Original and Three Replicas

IV. USE OF THE MODULATION TRANSFER FUNCTION TO ANALYZE TAG AUTHENTICATION

A. Introduction to the Modulation Transfer Function

It is essential to provide a first principle framework for analyzing indirect tag casting authentication. The modulation transfer function (MTF) provides such a framework. It is widely used to analyze the accuracy[4] of a variety of imaging-system components and whole imaging systems. For example, components such as particular film types or lens designs have an MTF associated with each of them. A camera is an example of an imaging system with an MTF determined by its lens and film MTFs. Tag authentication by SEM images of plastic castings also relies upon an imaging system. An original TLI surface tag is imaged by a system with two components. These components are the plastic casting and the SEM. A replicated surface tag is imaged by a four-component system. Different system MTFs can be determined for original or replicated tags.

The MTF is presented as a curve that quantifies the imaging accuracy of any imaging system or component as a function of the spatial frequency of the scene being imaged. For most systems, the MTF curve illustrates the common-sense notion that large spatial frequencies are imaged more accurately than small frequencies. The MTF is also known by the following names: contrast transfer function, sine wave response, and frequency response.

An understanding of the tag-imaging-system accuracy as it relates to the spatial frequencies being imaged is crucial for tagging. For instance, if the plastic casting made a totally inaccurate impression of the original tag surface it would be impossible to authenticate this surface by comparing casting images. The tag-surface image captured by a totally inaccurate plastic casting would not correlate well enough to discriminate the original surface imaged in the baseline examination from the image obtained in a subsequent field examination of the same surface. On the other hand, if the plastic casting made perfectly accurate copies of an original surface, it could be used to make perfectly accurate replicas of the surface. The tag-surface topography captured by a perfectly accurate casting could be used to form a perfectly accurate replica of the original surface. Subsequent castings made from either an original tag surface or a replica surface would correlate perfectly, and the tag would not be unique. Indeed, spatial frequency ranges that approximate totally inaccurate castings or perfectly accurate castings can be defined. Of course these ranges do not lead to a viable tag, and these spatial frequencies ranges are not used to define this tag.

The MTF is used to optimize the plastic-surface-casting tag to ensure its uniqueness. Specifically, the MTF defines a spatial-frequency range where the castings are accurate enough to authenticate an original (genuine) tag, but not accurate enough to make undetectable replicas of the original surface. It should also be emphasized that the MTF by itself does not provide a numerical image comparison necessary for tag authentication. The LCC and the local-sum mean must still be used to provide a numerical comparison. However, using the MTF leads to comparisons that provide the greatest numerical discrimination between castings made from an original surface and castings made from replicas of the original surface.

B. MTF Description

1. MTF Example

MTF curves are routinely determined and provided by the manufacturers of imaging-system components. For example, Fig. 7 presents the MTF of a particular type of photographic film (Kodak 2476). The abscissa can be thought of as the spatial frequencies on a sinusoidally varying gray-scale object being imaged in the film. The ordinate is the modulation transfer (MT) expressed in percent. The MT can be thought of as a numerical indication of how well the film reproduces a particular frequency. Examination of Fig. 7 shows that below a spatial frequency of ten cycles/mm the film image provides perfectly accurate object resolution. For frequencies near forty cycles/mm the film has a MT near 50%. This means that the film is midway between perfect accuracy and total inaccuracy for spatial frequencies near forty cycles/mm. At very high frequencies the MT approaches zero. So, for very high frequencies, the MT value indicates the film is approaching total inaccuracy. The physical reason for this inaccuracy is that the film cannot resolve features much smaller than its grain size. All imaging components have a zero MT for appropriately high spatial frequencies. For instance, even a theoretically perfect lens has a diffraction-limited spatial resolution.

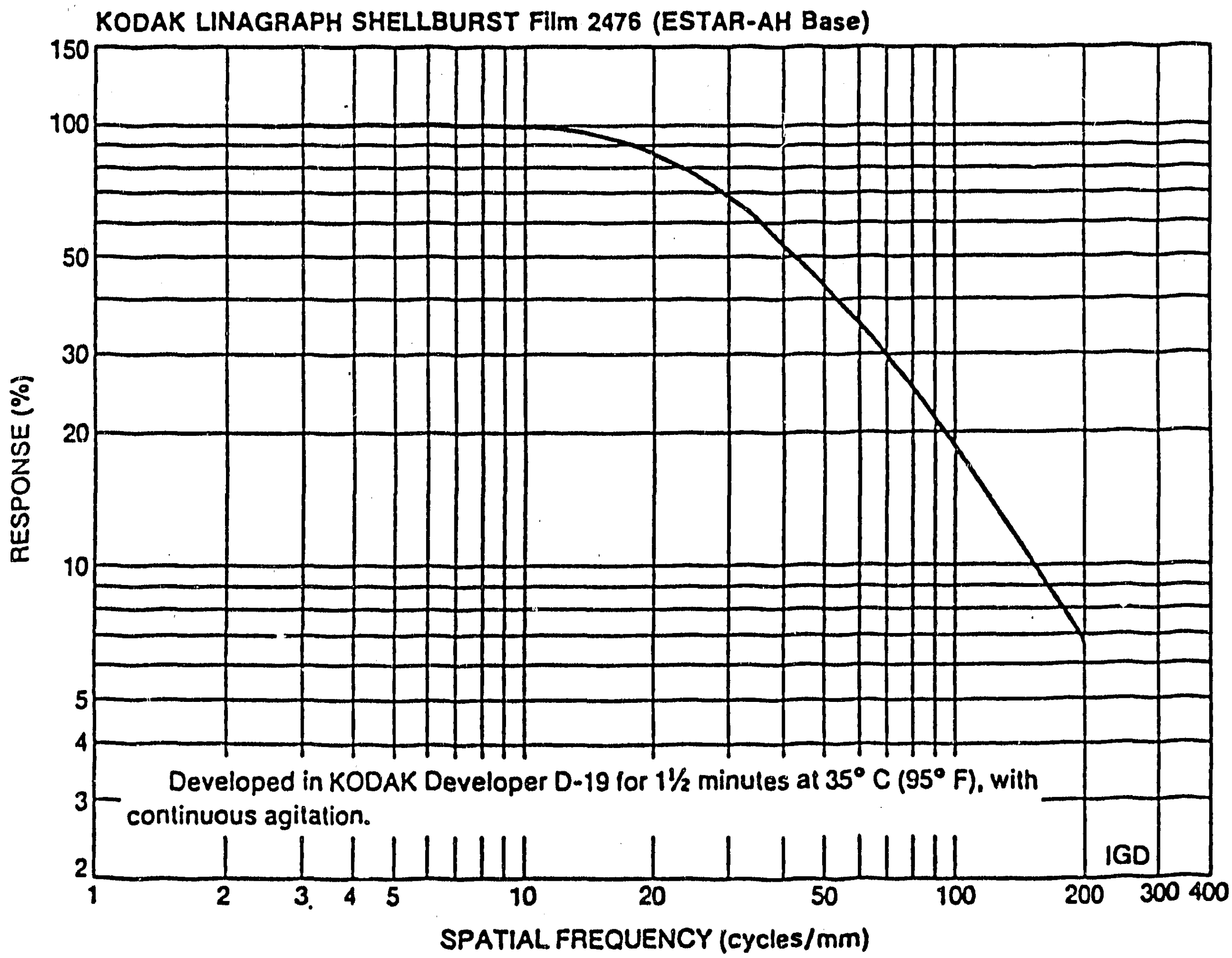

Figure 7. Sample MTF Curve for Photographic Film

2. MTF Definition

This subsection presents a simplified definition of the MTF. The MTF curve describes the dependence of the MT upon spatial frequency. At each frequency, the MT defines how the object's sinusoidal gray scale is transferred to the image.

The object's gray variation G_o in the x spatial coordinate has a sine dependence upon spatial frequency, f, according to:

$$G_o = O_1 + O_2 \sin (2\pi fx) \quad (1)$$

O_1 and O_2 are the constant and amplitude of the gray sine variation, respectively. The object modulation at spatial frequency f is defined as:

$$M_o(f) = O_2/O_1 \quad (2)$$

The image gray spatial variance is:

$$G_i = I_1 + I_2 \sin (2\pi fx) \quad (3)$$

I_2 and I_1 are the constant and modulus of the image's gray-scale sine variation, respectively. The image modulation M at spatial frequency f is:

$$M_i(f) = I_2/I_1 \quad (4)$$

The modulation transfer, MT, at spatial frequency f is:

$$MT(f) = M_i(f)/M_o(f) \quad (5)$$

The modulation transfer function, MTF, is the frequency dependence of the MT.

3. MTF System Product Rule

The MT of an imaging system at each frequency is the product of the MTs of its individual components at that frequency. The modulation transfer of a n-component imaging system, MT_{sys}, is:

$$MT_{sys} = \prod_{c=1}^{n} MT_c \quad (6)$$

For example, a camera is an optical system whose individual components are a film and lens. Therefore, at each frequency, the MT of the camera is the product of the film MT times the MT of the lens. The system MTF is then the function defining the frequency dependence of the system MT.

C. MTF-Optimized Tag Authentication

For either the baseline or the field inspection, the components of the imaging system used to image an original tag surface consist of a single plastic casting and an SEM. According to Eq. (6), the modulation transfer of the original (genuine) tag system, $MT_{or,sys}$, is:

$$MT_{or,sys} = MT_{ca}MT_{sem} \tag{7}$$

MT_{ca} is the casting modulation transfer, and MT_{sem} is the SEM modulation transfer. Since $MT_{or,sys}$ is determined for each spatial frequency, the modulation transfer function of the original tag system, $MTF_{or,sys}$, can be formed for all frequencies. Figure 8 graphically shows $MTF_{or,sys}$ as a product of the system component MTFs. This figure illustrates that the $MTF_{or,sys}$ is determined as a first-generation image of the original tag surface.

For a field inspection on a replicated tag, the components of the imaging system consist of a replicated negative made from the original tag, a replicated tag positive, a single plastic casting, and an SEM. According to the product rule, the modulation transfer of the replicated tag system, $MT_{rp,sys}$, is then:

$$MT_{rp,sys} = MT_{neg}MT_{pos}MT_{ca}MT_{sem} \tag{8}$$

MT_{neg} and MT_{pos} are the modulation transfers of the negative made from the original tag and the replicated tag positive, respectively. Figure 9 graphically shows $MTF_{rp,sys}$ as a product of its system component MTFs. This figure illustrates that the $MTF_{rp,sys}$ is determined from a third-generation image of the original tag surface. Figure 10 plots the original system and the replicated system MTFs from Figs. 8 and 9, respectively. It should be emphasized that these MTFs were not directly determined, but were approximated from the results of the replication experiments presented in Section II. Figure 10 indicates that the optimal spatial frequency range for tag authentication corresponds to the range $1 > MT_{or,sys} > 0$. In this range, $MT_{or,sys} > MT_{rp,sys}$, and the frequency is not beyond the resolving power of the genuine system. Figure 10 graphically expresses that a

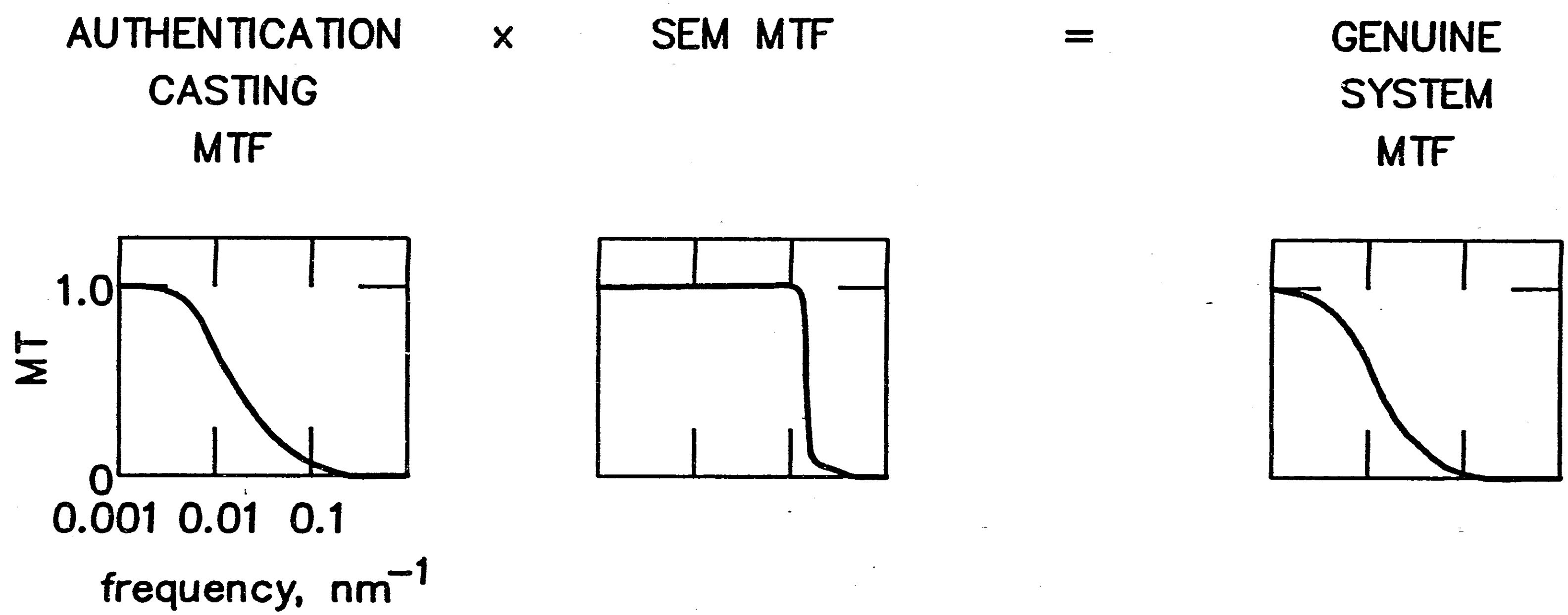

Figure 8. Original (Genuine) Tag MTF

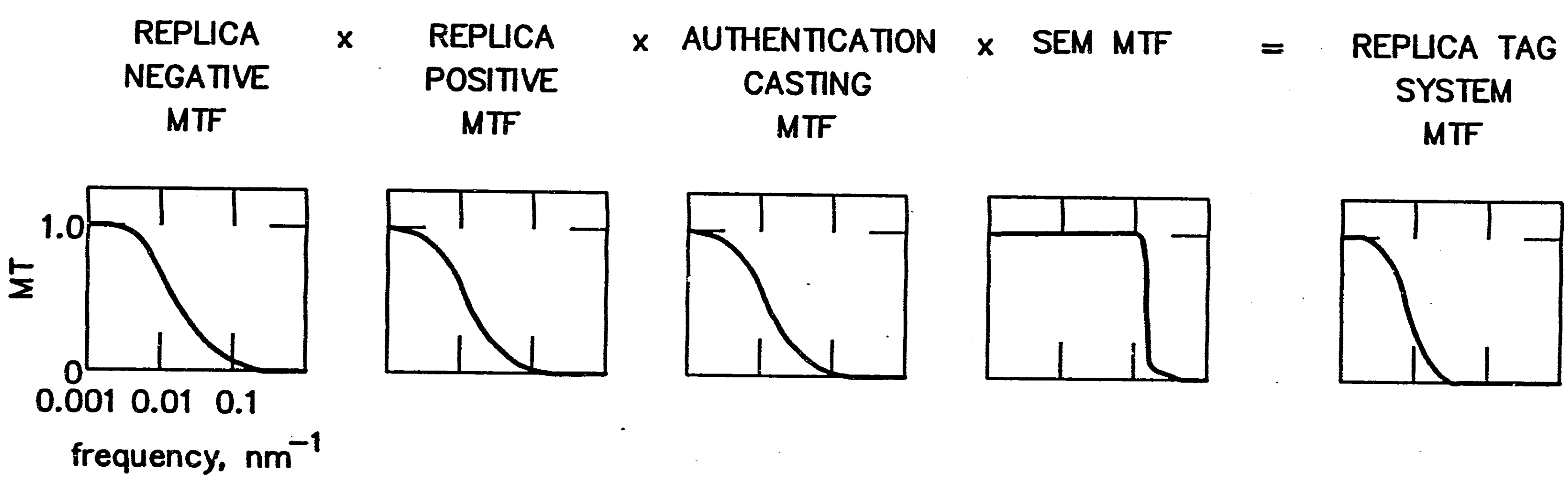

Figure 9. Replicated Tag MTF

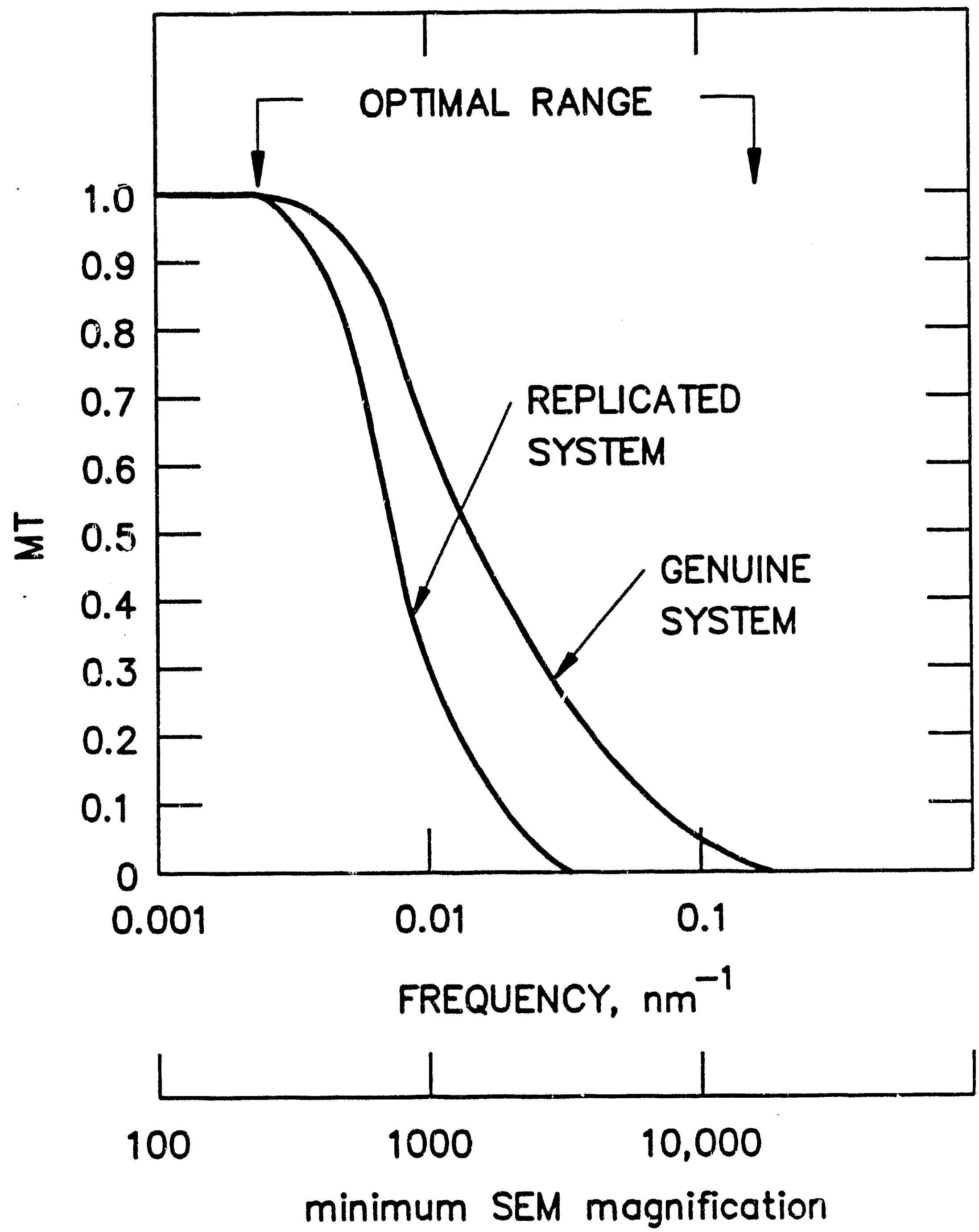

Figure 10. MTF Optimized Magnification and Features

third-generation plastic casting made from a replicated tag results in a lower system MT than the first-generation casting made from a genuine tag. Replication errors compound with each generation, and this is expressed by the inequality $MT_{or,sys} > MT_{rp,sys}$ in the optimal frequency range. The abscissa in Fig. 10 also shows a minimum SEM magnification that can resolve the spatial frequency. This brings in the need to operate the microscope in a magnification range likely to resolve significant differences between original and genuine tags.

Some simplifying approximations are now made to extend this analysis of MTF optimized tagging. If the negative made from the original tag, the replicated tag positive, and the plastic casting are assumed to have the same modulation transfer, then:

$$MT_{neg} = MT_{pos} = MT_{ca} \tag{9}$$

The justification for $MT_{neg} = MT_{ca}$ is that they both must be formed in the liquid state from a plastic material. A plastic is necessary, because the negative and the casting must be deformable enough to be separated from a microscopically rough surface in one piece. The replicated tag positive can also be formed from the liquid state. If it is formed from the liquid state, the approximation, $MT_{pos} = MT_{ca}$, can also be made.

Another approximation is to set the modulation transfer of the SEM to one in the range $1 > MT_{ca} > 0$.

$$MT_{sem} = 1 \tag{10}$$

The validity of this assumption depends upon the resolution of SEM used to image the casting. It is likely to be valid for a high-resolution field-emission SEM.

Combining Eqs. (9) and (10) with Eqs. (7) and (8) results in the following approximations to the system MTFs:

$$MT_{or,sys} = MT_{ca} \tag{11}$$

$$MT_{rp,sys} = MT_{ca}^{\ 3} \tag{12}$$

Optimization of the tag imaging conditions can be quantified by determining the maximum difference between $MT_{or,sys}$ and $MT_{rp,sys}$ as:

$$\frac{d}{d\,MT_{ca}}\left(MT_{or,sys} - MT_{rp,sys}\right) = 0 = 1\text{-}3MT_{ca}^{\ 2} \qquad (13)$$

The maximum difference occurs for a spatial frequency with a $MT_{ca} = 0.577$. Indeed, the range of spatial frequencies around this frequency also provide useful discrimination of genuine from replicate tags. Therefore, the tag is optimized for a range of spatial frequencies that correspond to MTs near 0.577. In other words, the most significant differences between castings made from an original and castings made from a replica occur for spatial frequencies in this range.

Since the MTF analysis determined a range of optimal spatial frequencies, it is now possible to state the particulars that result in a unique tag.

1. Select the tag marking device to maximize the density of the optimal spatial frequencies. For example, the grit size of the sandpaper used to form the tag's topography should be selected to maximize features with the optimal spatial-frequency range.

2. Select an SEM magnification that resolves the entire optimal spatial frequency range.

3. Compare the digital baseline and field-inspection images, with weighted spatial frequency. Zero weight would be given to spatial frequencies for $MT_{or,sys} = 1$ or $MT_{or,sys} = 0$. Maximum weight would be given to the frequency corresponding to the maximum difference in $MT_{or,sys} - MT_{rp,sys}$. This maximum weighted spatial frequency has an $MT_{ca} = 0.577$ under the approximations discussed in the derivation of this frequency. The linear correlation coefficient obtained from a frequency weighted image would have better tag discrimination than the unweighted LCC discussed in Section II. It may be possible to discriminate genuine from replicate tag images solely from the weighted LCC. Implementation of the spatial weighting is relatively straightforward, since the unweighted LCC is already determined in frequency (Fourier) space. A weighted LCC could easily be obtained from the Fourier transforms of the registered images.

D. Use of the MTF to Interpret Replication Experiments

1. SEM Magnification and Image Comparison

Table I presents the LCCs and the local-sum means for all the tag images compared in this study. Results for a range of magnifications between low (700X) and moderate (5500X) are presented. Both castings from original tags as well as original and replica images are compared. Some of the image comparisons in Table I were used to form the tag sub-area acceptance criteria presented in Section IIIB.

In Table I, six of the seven original versus replicated tag comparisons obtained from SEM magnifications at moderate SEM (5500X) magnification were discriminated by the tag authentication algorithm proposed in Section IIIB. Indeed, the local-sum mean quantitatively expresses the high spatial frequency defects visual to the eye at moderate magnification. This SEM magnification must be close to the MTF optimized magnification for tag discrimination discussed previously.

At lower SEM magnifications, the MTF analysis predicts that it would not be possible to discriminate original from genuine tags. This is because low magnification images do not contain enough information from the optimally discriminate spatial frequency range. Figure 11 shows a lower magnification view of an original (top) and two replicas of the same area. The SEM magnification used to obtain these images was 700X. Visual comparison of the replicas shows none of the bright ridge line imperfections visible at higher magnifications. The local-sum statistic, designed to evaluate bright features, does not discriminate between the original and the replicas at low magnification. The spatial frequencies resolved at the lower magnifications have a casting modulation transfer nearly equal to one, so the difference in modulation transfer between the original and replica is very small.

It is necessary to modify the standard formulation of the modulation transfer function to explain the one original-replica sub-area comparison presented on the left side of Fig. 12. Figure 12 shows a pair of original-replica comparisons from the same replica. Both comparisons are of small sub-areas, and the sub-areas are only ten microns apart. The left hand image comparison was the only replica image at 5500X that met the authentication criteria proposed in Section IIIB. Note the right-hand original-replica

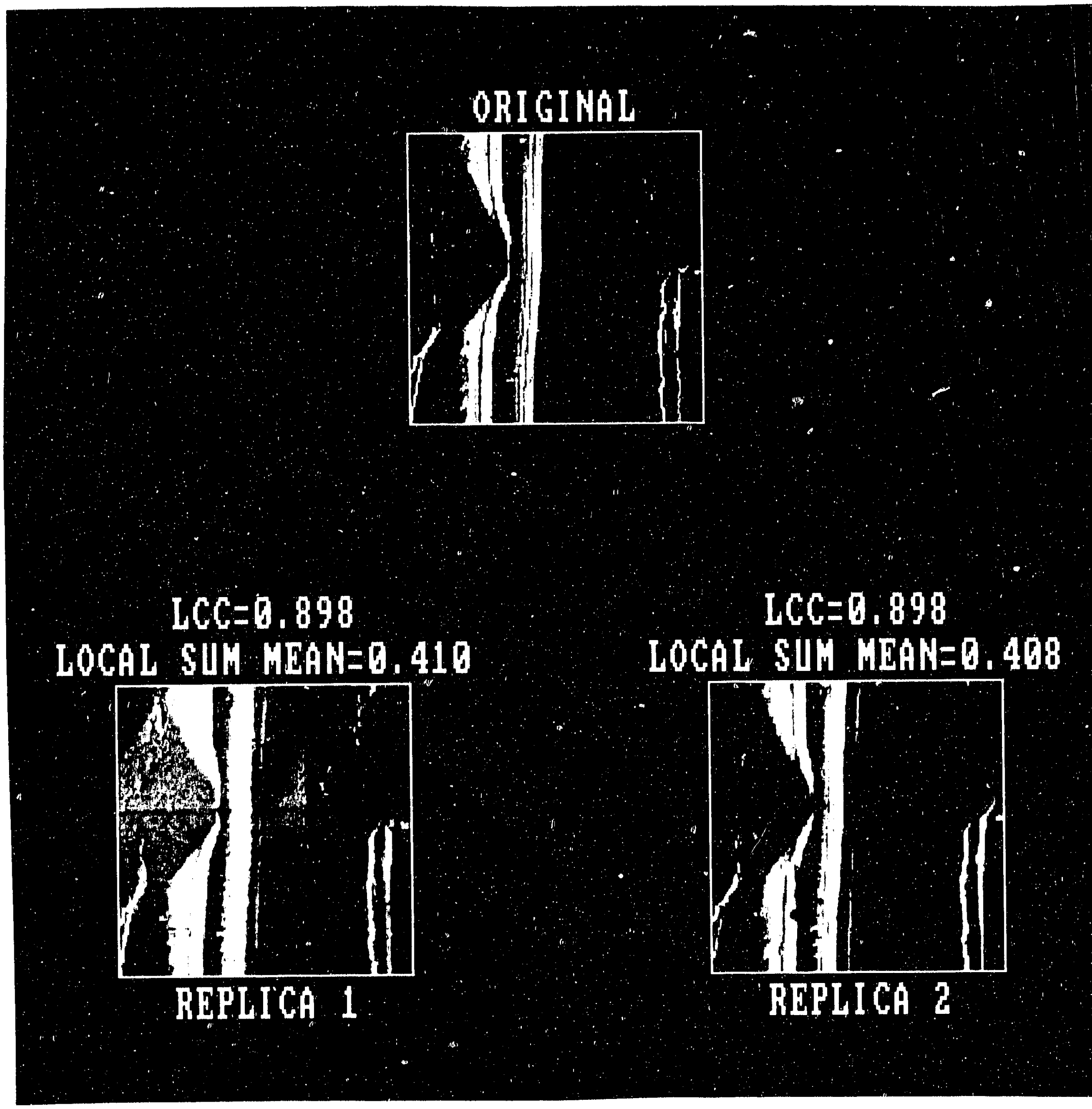

Figure 11. Original and Two Replicas at Low Magnification

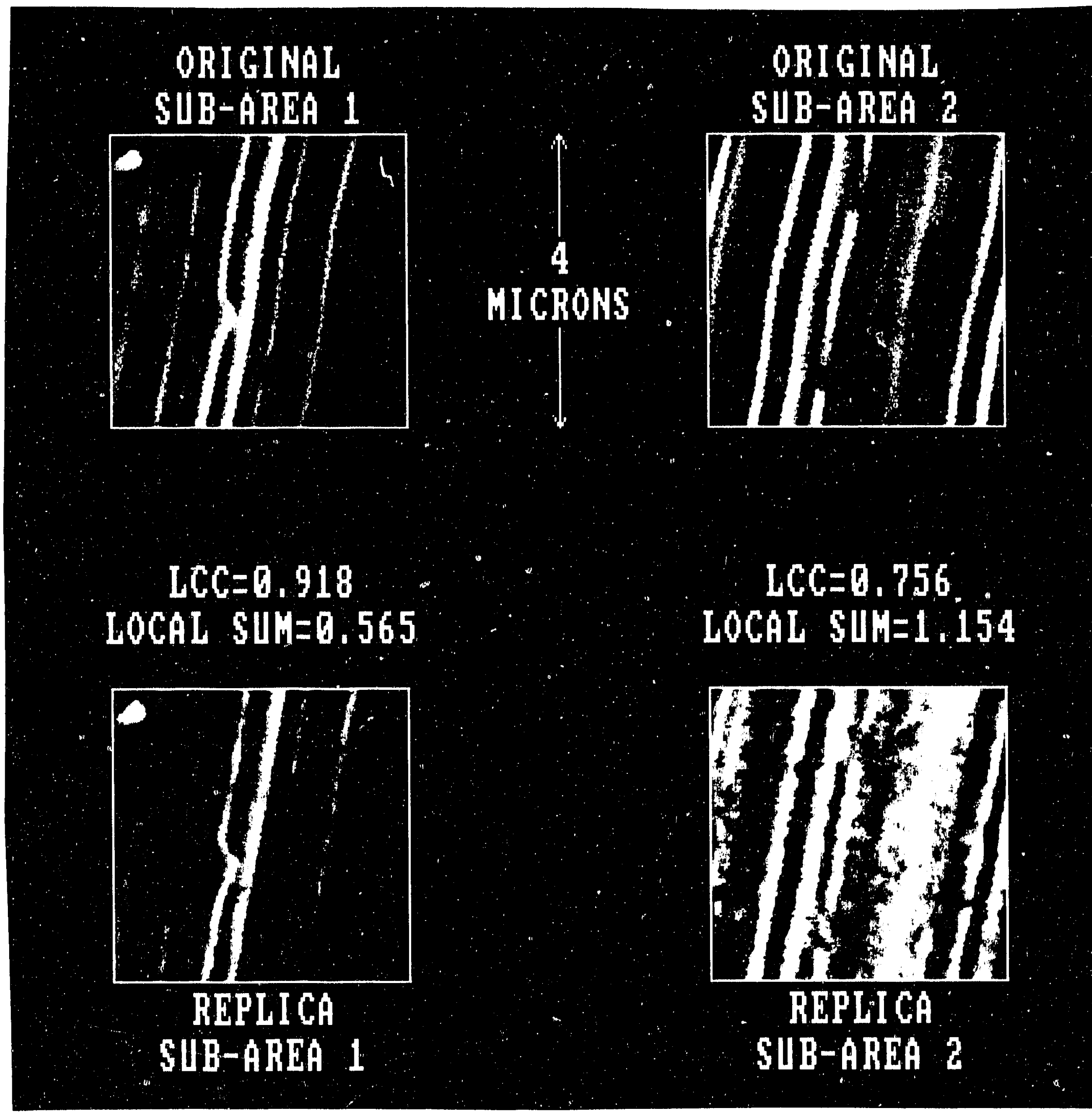

Figure 12. Comparison of Two Nearly Adjacent Sub-Areas

sub-area comparison in Fig. 12 failed to meet the acceptance criteria. The right hand area was only eleven microns away from the left-hand sub-area that met the criteria. It is plausible that local sub-area replication accuracy is dependent upon a combination of tag-surface topography, casting solute/solvent ratio, or other factors. If this is true, then the cellulose-acetate, casting modulation transfer may fall-off as a band of values when $MT_{ca} < 1$ rather than as a single value at each frequency. Therefore, the excellent replica sub-area in Fig. 12 was produced by a negative casting that had a local sub-area MTF at the top of the MTF band. MTF analysis predicts it would be possible to detect that the sub-area on the left side of Fig. 12 as a replica by examining it at higher magnification. It is important to note that each of the sub-areas represent only 0.000016% of the one square centimeter tag area. Most of the sub-areas in a original-replica comparison are expected to fail to meet the acceptance criteria. A tag's authenticity must be based upon comparisons from several sub-areas.

The slope of the $MTF_{or,sys}$ curve with frequency in the range $1 > MT_{or,sys} > 0$ is an important consideration for implementing MTF optimization. It is desirable to have a slightly negative slope, so there will be a wide range of optimal spatial frequencies for tag discrimination. Figure 13 shows the same casting sub-area imaged at magnifications of 1000, 2000, and 4000X. Figure 14 shows another casting sub-area imaged at magnifications of 4000, 8000, and 16000X. Examination of Figs. 13 and 14 reveals that tag-image sharpness slowly degrades with increasing magnification. These figures provide qualitative assurance the slope of $MTF_{or,sys}$ with spatial frequency is slightly negative.

It is important to note that the MTF only addresses random differences between castings. Systematic differences between the original and replicate tags have also been observed. An example of a systematic difference is the presence of rounded micro-bubbles features in the replica surface. Micro-bubbles have been observed in negative replication. Systematic differences would reside in the same location in two or more castings made from a replica. However, systematic differences would not be present at the same location in multiple castings made from an original tag. It may be also possible to discriminate castings made from originals and replicas based upon systematic defects.

V. CONCLUSIONS

Numerical authentication criteria for a unique intrinsic-surface tag were formulated. These criteria were based upon experiments and a first principle's analysis.

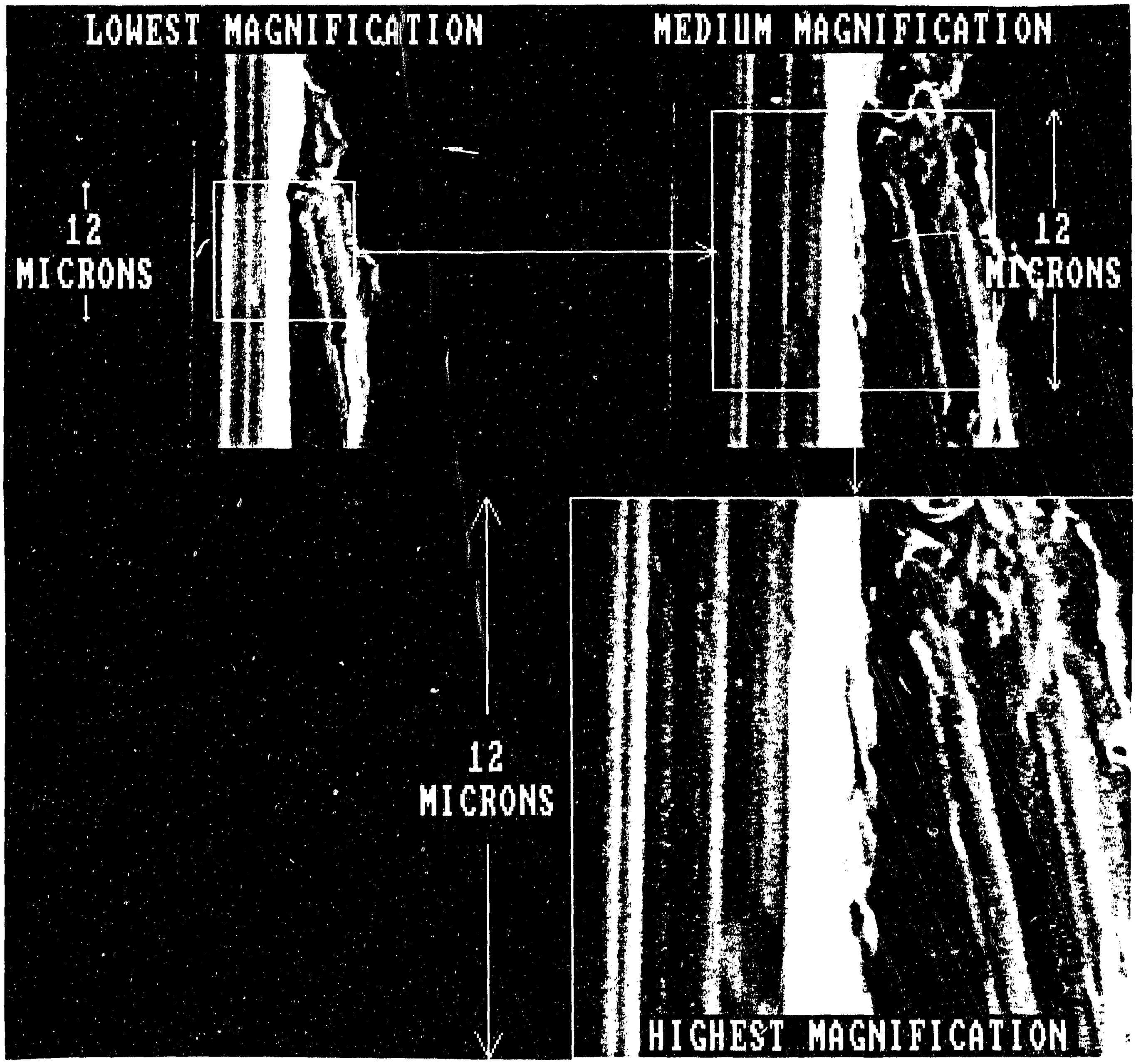

Figure 13. Same Casting Imaged at Magnifications of 1000, 2000, and 4000

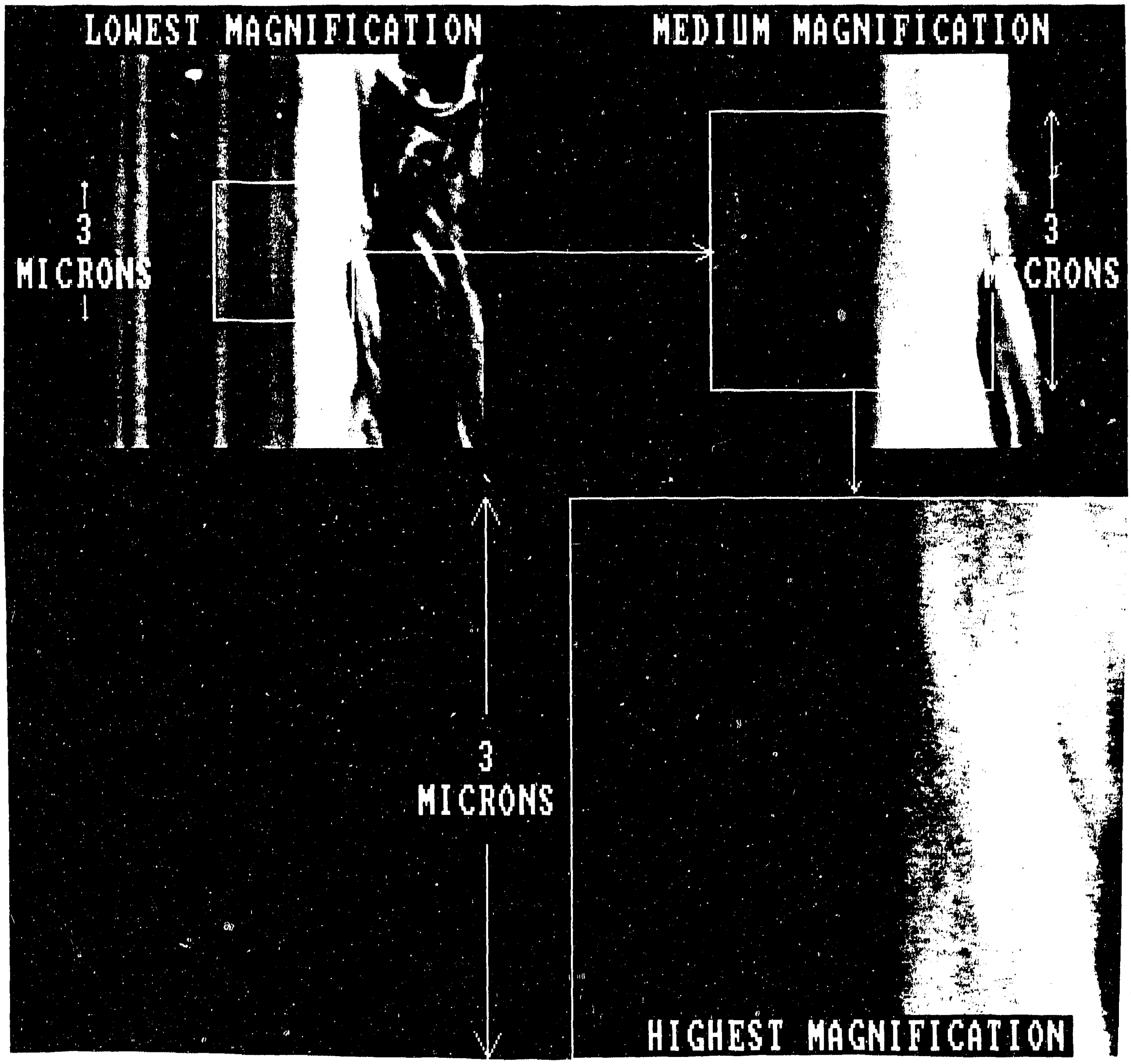

Figure 14. Same Casting Imaged at Magnifications of 4000, 8000, and 16000

Surface replication experiments showed the linear correlation coefficient must be supplemented with another statistic in order to numerically discriminate original from replica surfaces. This additional statistic was called the local sum, and it was empirically formulated. The local sum statistic provided sensitivity to bright, high-spatial-frequency defects in the replicas.

The modulation transfer function, a first principle's imaging concept, was used to analyze the surface replication results. This function revealed how the surface uniqueness is optimized for a specific spatial-frequency range. Both the tag's surface topography and authentication magnification must be chosen to emphasize features in the optimal range. In addition, a linear correlation coefficient, weighted to emphasize only optimal-range surface features, could provide increased discrimination ability.

REFERENCES

1. O. S. Crankshaw, Instruction of Replica Techniques for Scanning Electron Microscopy, Scanning Electron Microscopy, No. IV, 1731-1737 (1984).

2. J. H. M. Willison and A. J. Rowe, Practical Methods in Electron Microscopy, Vol. 8, Replica, Shadowing, and Freeze-Etching, North-Holland Publishing Company, Amsterdam (1980).

3. A. DeVolpi, "Understanding Correlation Coefficients in Treaty Verification," Argonne National Laboratory report, ANL/ACTV-91/4 (1991).

4. W. J. Smith, Modern Optical Engineering, McGraw-Hill, New York (1966).

Appendix I

Semper Image Processing Software

A. INTRODUCTION

The gray-scale and binary-image processing has been implemented in the Semper 6.2 image processing software. This software is a trademark of Synoptic's Ltd. Semper is a general-purpose image processing program. Commands used for such diverse image-processing tasks as correlation, particle-size analysis, remote sensing of satellite images illustrate a sampling of Semper's capabilities. The commands can be entered individually in the interactive mode, or interpreted programs can be written using the commands and the logical testing capabilities provided in the Semper language. Interpreted programs for correlation and local-sum mean calculation are described in this Appendix.

B. IMAGE REGISTRATION AND CORRELATION

An image matching tag must register two as-acquired source images using image correlation. For two digital images, registration is achieved when the x,y addresses of each image correspond to the same points on the surface being compared. In general, two digital images of the same or similar surfaces are dissimilar if the imaging device or the surface moves between acquiring the images. These dissimilarities can be described either as translation, rotation, or magnification differences. In the case of digital tag images acquired by a scanning electron microscope all these differences must be corrected before the tag can be scored. The registration software calculates many linear correlation coefficient (LCC) values as it searches for the minimum difference. The LCC is maximized at the minimum difference. This maximum LCC is also used as part of the tag score. Most of the computational effort (~90%) to score the tag is spent in registering the images.

A program has been written that uses several Semper commands to accomplish registration or overlay by image correlation. The Semper software uses standard Fourier techniques to accomplish registration. Fourier techniques are used because they are more computationally efficient for the large size images being compared. The most important Semper correlation command (XCF), translates two images over each other and reports the Δx and Δy translations that provide the best registration. The best overlay is determined from the peak linear correlation coefficient amongst all the translations. In general, N^2 registration correlations are calculated for input images of size N by N. Another Semper correlation command (OCF) determines the rotational correlation between two images. OCF, as implemented in this program, operates on the real images but can also be implemented on their Fourier power spectra. The last important Semper routine (EXTRACT) extracts a translated, magnified, and rotated sub-image from an as-acquired image using bilinear interpolation.

The program implements registration in the following manner. One input sub-image (e.g., 128 x 128 pixel size) is simply extracted from the first source image, which is typically a 512 x 512 pixel image. The second sub-image is constantly being extracted from the second source image. This program attempts to find the optimum extraction of the second sub-image. This extraction is determined by the search for peak registration of the two sub-images, and it is accomplished in three steps. The first step determines a translation registered second sub-image. This image is used to start the magnification search in the second step. A translation and magnification registered second sub-image is determined upon concluding this step. This sub-image is used as input to the third step. The third step corrects for rotational differences. The output of the third step is the maximum LCC between the first and second sub-images since it has been corrected for all differences. This correlation is computed to within a 0.5 pixel shift and a 0.1 degree rotation of the theoretically best registration. It provides a maximum LCC accurate to at least the third decimal point of the theoretically best registration. It is important to note the casting images could be overlaid by a less computationally intensive process. However, overlay of the original and replica images was complicated by the presence of false maximum correlations, so more calculations were required to assure that the true maximum was found. Another important detail is that the magnification and rotation steps sometimes require an additional translation correction to maximize the LCC. If this is required, an additional translation correction is implemented within the magnification and rotation steps.

Table A-I of this report gives the Semper code source listing for the correlation program MATCHIM, and Table A-II gives a sample output for this program.

TABLE A-I

SEMPER SOURCE FOR IMAGE CORRELATION PROGRAM MATCHIM

```
Matchim()
TIME RESET
PAGE NOPROMPT
!PROGRAM MATCHIM IS WRITTEN TO OVERLAY TWO IMAGES
!WITH STRONG DIRECTIONAL COMPONENTS SUCH AS IMAGES
!OF SCRATCHES RUNNING IN ONE DIRECTION.
!NOTE THE IMAGES ALSO NEED A STRONG DIRECTIONAL COMPONENT.

LOCAL SZ1,II1,XX1,XX2,IO1,II2,XX2,YY2,IO2,TP,TM,TRP,TRM
LOCAL T1,T2,T3,T4,T5,A,B,KE,KRE,SZ2,SF1,ORD,IRD,TH1,TH2,DEL
LOCAL X2,Y2

ASK 'SIZE OF OVERLAID OUTPUT IMAGES?  ' SZ1

!FIRST OUTPUT IMAGE EXTRACTED FROM FIRST INPUT
!IMAGE AT INPUT COORDINATES.

ASK 'FIRST INPUT IMAGE FOR OVERLAY  ' II1
ASK 'X,Y POSITION IN FIRST INPUT IMAGE  ' XX1,YY1
ASK 'OUTPUT IMAGE NUMBER AS EXTRACTED FROM FIRST IMAGE  ' IO1

!SECOND OUTPUT IMAGE IS EXTRACTED FROM SECOND
!INPUT IMAGE AFTER OPTIMUM SHIFT, MAGNIFICATION
!AND ROTATION CORRELATION IS DETERMINED.

ASK 'SECOND INPUT IMAGE FOR OVERLAY  ' II2
ASK 'X,Y POSITION IN SECOND INPUT IMAGE  ' XX2,YY2
ASK 'OUTPUT IMAGE NUMBER FROM SECOND IMAGE  ' IO2
X2=XX2
Y2=YY2
DEL 4001,4999

COPY II2 4001

CREATE 4002 SIZE SZ1 BYTE
EXTRACT II1 4003 SIZE SZ1 POS XX1,YY1
ORIGEN 4003 RESET
COPY 4003 IO1
FOU 4003

TYP 'DOING INITIAL SHIFT SEARCH FOR A COMMON CENTRAL PIXEL'
FOR K=1,5
  EXTRACT 4001 4002 SIZE SZ1 POSITION XX2,YY2
  ORIGEN 4002 RESET
  XCF 4003 WITH 4002 TO 4990
  IF X=0 & Y=0 JUMP MG1
  XX2=XX2+X
  YY2=YY2+Y
LOOP
TYP 'CAN'T GET X=Y=0 SHIFT CORRELATION IN 5 TRIES, X,Y= ',X,Y
```

TABLE A-I (continued)

SEMPER SOURCE FOR IMAGE CORRELATION PROGRAM MATCHIM

```
MG1:
! T1 IS TMAX FOR INITIAL SHIFTING
T1=T

TYP 'DOING MAGNIFICATION ADJUSTMENT'
A=1
EXTRACT 4001 4002 SIZE SZ1 POSITION XX2,YY2 SAMPLING (1+(.5/SZ1))
ORIGEN 4002 RESET
XCF 4003 WITH 4002 TO 4990
TP=T

EXTRACT 4001 4002 SIZE SZ1 POSITION XX2,YY2 SAMPLING (1-(.5/SZ1))
ORIGEN 4002 RESET
XCF 4003 WITH 4002 TO 4990
TM=T

IF TP<TM A=-1

T2=T1
SZ2=ROUND(SZ1/8)
FOR K=1,SZ2
  KE=K
  EXTRACT 4001 4002 SIZE SZ1 POSITION XX2,YY2 SAMPLING +
  (1+((A*K)/SZ1))
  XCF 4003 WITH 4002 TO 4990
  XX2=XX2+X
  YY2=YY2+Y
  IF T<T2 JUMP MG2
  ! NOTE WHEN K=KE-1, T=TMAX, SO T2=TMAX AT JUMP TIME
  T2=T
LOOP
TYP 'UNABLE TO FIND MAGNIFICATION ADJUSTMENT, WITHIN 12% LIMIT'
RETURN

MG2:

! TYP 'DOING FINE MAGNIFICATION ADJUSTMENT'
SF1=1+((A*(KE-1))/SZ1)
! SF1 ABOVE IS THE SAMPLING FACTOR THAT GAVE
! THE PEAK CORRELATION IN LABEL MAG1
! WHICH PROVIDED CRUDE MAGNIFICATION ADJUSTMENT
SF1=SF1+.5/SZ1
EXTRACT 4001 4002 SIZE SZ1 POSITION XX2,YY2 SAMPLING SF1
ORIGEN 4002 RESET
XCF 4003 WITH 4002 TO 4990
T3=T
IF T3>T2 JUMP ROT

SF1=SF1-1.0/SZ1
EXTRACT 4001 4002 SIZE SZ1 POSITION XX2,YY2 SAMPLING SF1
ORIGEN 4002 RESET
XCF 4003 WITH 4002 TO 4990
T3=T
IF T3>T2 JUMP ROT
```

TABLE A-I (continued)

SEMPER SOURCE FOR IMAGE CORRELATION PROGRAM MATCHIM

```
SF1=SF1+.5/SZ1
EXTRACT 4001 4002 SIZE SZ1 POSITION XX2,YY2 SAMPLING SF1
ORIGEN 4002 RESET
T3=T2

ROT:


TYP 'DOING ROTATIONAL CORRELATION, INITIAL OCF ANGLE FOLLOWS:'
! T3 AND SF1 ARE SET COMING INTO ROTATE AS THE PEAK
! CORRELATION AFTER MAGNIFICATION ADJUSTMENT,
! AND THE SAMPLING FACTOR THAT PROVIDES THE
! PEAK CORRELATION.
ORD=(SZ1/2)-1
IRD=1
OCF IO1 WITH 4002 TO 4999 FULL RINGS 25 RAD IRD,ORD VER
TYP 'OCF THETA= ',DEG(THETA),' DEGREES ',THETA,' RADIANS'

TH1=THE
DEL=(.1/180)*PI
B=1

EXT 4001 4002 SIZ SZ1 POS XX2,YY2 SAM SF1 ANG TH1
ORIGEN 4002 RESET
XCF 4003 WITH 4002 TO 4990
T4=T
EXT 4001 4002 SIZ SZ1 POS XX2,YY2 SAM SF1 ANG TH1+DEL
ORIGEN 4002 RESET
XCF 4003 WITH 4002 TO 4990
TRP=T

EXT 4001 4002 SIZ SZ1 POS XX2,YY2 SAM SF1 ANG TH1-DEL
ORIGEN 4002 RESET
XCF 4003 WITH 4002 TO 4990
TRM=T
IF TRP<TRM B=-1

T5=T4
FOR K=1,15
  KRE=K
  EXT 4001 4002 SIZ SZ1 POS XX2,YY2 SAM SF1 ANG (TH1+B*K*DEL)
  ORIGEN 4002 RESET
  XCF 4003 WITH 4002 TO 4990
  IF T<T5 JUMP DONE
  T5=T
  XX2=XX2+X
  YY2=YY2+Y
LOOP

TYP 'COULDN'T FIND ANGLE TO ROTATE OPTIMALLY IN 15 TRIES'
TYP 'XX2,YY2= ',XX2,YY2,' T5= ',T5
TYP 'XX2,YY2= ',XX2,YY2,' T5= ',T5
```

TABLE A-I (continued)

SEMPER SOURCE FOR IMAGE CORRELATION PROGRAM MATCHIM

```
DONE:


TH2=TH1+B*(KRE-1)*DEL
EXT 4001 4002 SIZ SZ1 POS XX2,YY2 SAM SF1 ANG TH2
ORIGEN 4002 RESET
COPY 4002 IO2

TYP ''
TYP 'FINAL CORRELATION AFTER MAGNIFICATION+ROTATION= ', T5
TYP 'INITIAL SHIFT, FINAL MAGNIFICATION CORRELATIONS ', T1,',',T3
TYP 'OUTPUT IMAGE SIZE, FINAL SAMPLING(1/MAG.) FACTOR= ', SZ1,',',SF1
TYP 'FINAL X,Y EXTRACTION COORDINATES FOR SECOND IMAGE= ', +
XX2,',',YY2
TYP 'FINAL ROTATION ANGLE ',DEG(TH2),' DEGREES  ',TH2,' RADIANS'
TYP ''
TYP 'EXAMINE FIRST INPUT IMAGE'
EXAMINE II1
TYP +
'INITIAL+FINAL X,Y COORDINATES FOR FIRST INPUT IMAGE ',XX1,',',YY1
TYP 'FIRST OUTPUT IMAGE NUMBER, ',IO1
TYP ''
TYP 'EXAMINE SECOND INPUT IMAGE'
EXAMINE II2
TYP 'INITIAL X,Y COORDINATES FOR SECOND INPUT IMAGE ',X2,',',Y2
TYP 'SECOND OUTPUT IMAGE NUMBER ',IO2
TYP ''
TYP +
'ESC INDICES FROM MG1,ROT; A,B SEARCH DIR VAL ',KE,'+
',KRE,';',A,',',B
TIME NOVER
TYPE 'PROGRAM TIME= ',FIX(T/60),' MIN  ',REM(T,60),' SEC'
PAGE PROMPT
end
```

TABLE A-II

SAMPLE OUTPUT OF SEMPER PROGRAM MATCHIM

```
FINAL CORRELATION AFTER MAGNIFICATION+ROTATION= 0.904789
INITIAL SHIFT, FINAL MAGNIFICATION CORRELATIONS 0.875711,0.903493
OUTPUT IMAGE SIZE, FINAL SAMPLING(1/MAG.) FACTOR= 128,0.980469
FINAL X,Y EXTRACTION COORDINATES FOR SECOND IMAGE= -7,95
FINAL ROTATION ANGLE -0.466315 DEGREES -0.00813874 RADIANS

EXAMINE FIRST INPUT IMAGE
 5041 Size 641, 480, 1 300.5kb Image Byte wp
    j814000
INITIAL+FINAL X,Y COORDINATES FOR FIRST INPUT IMAGE -96,47
FIRST OUTPUT IMAGE NUMBER, 5941

EXAMINE SECOND INPUT IMAGE
 5042 Size 641, 480, 1 300.5kb Image Byte wp
    j824000
INITIAL X,Y COORDINATES FOR SECOND INPUT IMAGE -8,95
SECOND OUTPUT IMAGE NUMBER 5942

ESC INDICES FROM MG1,ROT; A,B SEARCH DIR VAL 4,3;-1,-1
PROGRAM TIME= 9 MIN 45.45 SEC
```

C. LOCAL-SUM PROGRAM

The local-sum mean program LOCSUM is set up to prompt for two registered input gray-scale images, and for the percent of the brightest pixels desired in the thresholded images. The program then searches the histograms of the input images to provide binary images thresholded closest to the desired brightness percent. There is a minor implementation problem since, in general, the binary images will not have exactly the same brightness percentage, nor will either brightness percentage be equal to that requested in the input. Typically, if 15% brightness is used as the desired input threshold value, then the binary images might have 14-16% of their pixels set to one. These different percentages of bright pixels causes minor increases in the means of the absolute difference and local-sum images. However, this implementation problem does not affect the ability of the means to discriminate real from replica tag sub-regions.

After the binary images are obtained, the steps necessary to calculate the mean of the absolute-difference image and the local-sum image are straightforward.

Table A-III of this report is the Semper code source listing for program LOCSUM, and Table A-IV presents a sample output for this program.

TABLE A-III

SEMPER SOURCE FOR BINARY IMAGE PROCESSING PROGRAM LOCSUM

```
Locsum()
TYP 'THIS PROGRAM CALCULATES THE LOCAL-SUM MEAN FROM TWO GRAY'
TYP 'IMAGES THRESHOLDED TO THE BRIGHTEST FRAC OF PIXELS'
del 4001,4999
ASK 'IMPUT IMAGES TO THRESH. ,BRIGHTEST FRAC. TO THRESH. 'II1,II2,BT
! need histogram to develop threshold
HISTOGRAM II1 TO 4101 FP
! max,mn1 is min pixel value in imput image
MN1=MIN
! max is maximum gray level in input image
! d1 is size of histogram file
D1=MAX-MIN+1
!pcb sets nco and nro of input image
PCB II1
!extract out only the histogram part of the histogram file
!last two values in histogram file are min,max, respectively
EXT 4101 SIZ D1,1 LEF
!next steps integrate the histogram starting at the lowest gray value
SUM=0
FOR I=0,D1-1
 SUM=SUM+P(I)
 P I=SUM
LOOP
!next step normalizes the integration so values are from 0 to 1
CAL 4:101/(NRO*NCO)
!next step produces a file peaked at desired brightness fraction
CAL 1-MOD(4:101-(1-BT)) TO 4102
! peak command records the peak position in plist 4103
PEAK 4102 4103
!xh1 is x address of peak
XH1=P(0,0,0)
!mn1+xh1 give the desired gray level to attain a binary
!thresholded to the brightest bt1 fraction
CAL :II1>(MN1+XH1) TO 4104
SEL 4101
AB1=P(XH1)
DEL 4101,4103
COPY 4104 BYTE
COM DEV 4 NOVER
```

TABLE A-III (continued)

SEMPER SOURCE FOR BINARY IMAGE PROCESSING PROGRAM LOCSUM

```
!GET THRESHOLDED IMAGE FOR II2
HISTOGRAM II2 TO 4105 FP
MN2=MIN
D2=MAX-MIN+1
EXT 4105 SIZ D2,1 LEF
SUM=0
FOR I=0,D2-1
  SUM=SUM+P(I)
  P I=SUM
LOOP
CAL 4:105/(NRO*NCO)
CAL 1-MOD(4:105-(1-BT)) TO 4106
PEAK 4106 4107
XH2=P(0,0,0)
CAL :II2>(MN2+XH2) TO 4108
SEL 4105
AB2=P(XH2)
DEL 4105,4107
COPY 4108 BYTE
COM DEV 4 NOVER

!AT THIS POINT 4104 AND 4108 CONTAIN THE BINARY IMAGES
!THAT THE LOCAL-SUM MEAN WILL BE CALCULATED FROM
!CALCULATE ABSOLUTE DIFFERENCE BINARY FROM BRIGHTNESS THRESHOLDED
!BINARIES
CAL MOD(4:104-4:108) TO 4009
SURVEY 4009 FULL NOVER
MAD=MEA

!CREATE KERNAL LOCAL PIXEL WEIGHTING IMAGE TO USE WITH FIR COMMAND
CREATE 4010 SIZE 3,3 VALUE 1

!FORM LARGE LOCAL-SUM IMAGE
FIR 4009 TO 4011 WITH 4010
!EXTRACT A LOCAL-SUM WITHOUT BORDER PIXELS OF LARGE LOCAL-SUM IMAGE
EXT 4011 SIZ NCO-2,NRO-2
SURVEY 4011 FULL NOVER
MLS=MEA

TYP ''
TYP 'LOCAL-SUM MEAN= ',MLS
TYP ''
TYP 'MEAN ABS DIFF IMAGE= ',MAD
TYP 'ACTUAL BRT THR IMAGES 1 AND 2 ARE = ',1-AB1,1-AB2
end
```

TABLE A-IV
SAMPLE OUTPUT OF SEMPER PROGRAM LOCSUM
LOCAL-SUM MEAN= 0.586357 MEAN ABS DIFF IMAGE= 0.0649414 ACTUAL BRT THR IMAGES 1 AND 2 ARE = 0.151245 0.143188

DISTRIBUTION FOR ANL/ACTV-91/5

Internal:

ANL Contract Copy
ANL Patent Department
ANL Technical Publications Services (3)
A. Travelli (4)
R. G. Palm (76)

External:

U.S. Department of Energy Office of Scientific & Technical Information (12)
Manager, U.S. Department of Energy Chicago Operations Office
ANL Libraries (2)

DATE
FILMED
7/22/92